Differentiation of Prostate Cancer Cells by Using Flexible Fluorescent Polymers

Michael D. Scott,[a] Rinku Dutta,[a] Manas Haldar,[a] Bin Guo,[a] Daniel L. Friesner[b] and Sanku Mallik[*a]

[a]Department of Pharmaceutical Science,
[b]Department of Pharmacy Practice,
North Dakota State University, Fargo, ND 58102, USA

Sanku.Mallik@ndsu.edu

Supporting Information

Table of Contents

Monomer, Polymer Synthesis and Characterization:

The synthesis and characterization of the monomers are already reported.[1] Polymerization was performed in degassed DMF at 60 ºC. Upon purification via drop-wise addition of ethyl acetate, the polymers were characterized (**Table S-1**) using gel permeation chromatography (Waters 2690) with a refractive index detector and N, N-dimethylformamide as the solvent.

Table S-1. This table shows the results of the GPC.

Polymer	**Mw**	**Mn**	**P.I.**	**Concentration Used (nM)**
P2	114,428	78,161	1.46	27
P1	117,191	64,577	1.81	31

***Cell Culture Studies*:**

22Rv1 is a prostate cancer cell line derived from a human prostatic carcinoma xenograft, CWR22R.[2] This cell line represents both primary and relapsed cancer and is androgen-dependent.[2] Although, this cell line is an androgen presenting cell-line, it (like PC-3) does not respond well with hormonal treatment.[3] However, it has been reported that it can be inhibited by using a glycogen synthase kinase-3 (GSK-3) inhibitors. For example, SB216763 was reported by Kypta group, to inhibit growth and proliferation of 22Rv1 cells.[4] However, due to GSK-3 inhibitors potential side effects they such agents should only be used in special cases were they are likely to be effective. This cell line was grown in RPMI media (10% FBS and 1% antibiotics) and taken through three splitting cycles. Subsequently, the media was replaced with a dye-free RPMI. After two splittings, the cells were grown until confluent before culturing the media for fluorescence experiments.

PC-3 is an aggressive prostate cancer cell line. Due to the lack of androgen presenting cells, they do not respond to hormonal treatments. It is unlikely they would respond to GSK-3 inhibitors, which act by phosphorylation of the androgen presenting cells.[4] Differentiation between 22Rv1 and PC-3 cells would allow for the development of a low-cost, effective strategic therapeutic plan. This cell line was grown in RPMI media (10% FBS and 1% antibiotics) and taken through three splitting cycles. Subsequently, the media was replaced with a dye-free RPMI. After two splittings, the cells were grown until confluent before culturing the media for fluorescence experiments.

PANC-1 is a human pancreatic cancer isolated from a 56 year old male.[5] This cancerous cell line was used as a control to demonstrate that our polymer system could differentiate between prostate cancers from non-prostate cancer. This cell line was grown in DMEM media (10% FBS and 1% antibiotics) and taken through three splitting cycles. Subsequently, the media was replaced with a dye-free DMEM. After two splittings, the cells were grown until confluent before culturing the media for fluorescence experiments.

HEK-293 is a human embryonic kidney cell line. This non-cancer cell line has been reported to secrete some amounts of MMP-9.[6,7] This cell line will show that it is possible for our system to differentiate between non-cancerous cells from cancerous cells. This cell line was grown in MEM media (10% FBS and 1% antibiotics) and taken through three splitting cycles. Subsequently, the media was replaced with a dye-free MEM. After two splittings, the cells were grown until confluent before culturing the media for fluorescence experiments.

Upon the cells reaching a confluent state in their respective dye-free media, they were then aseptically transferred into a sterile centrifuge tube and centrifuged for 8 minutes at 1500 RPM. Supernatant was then removed and used for the fluorescence and ELISA experiments. Additionally, the RPMI, DMEM and MEM media before cell culture were used as the controls for fluorescence experiments.

Fluorescence Spectroscopic Studies:

The polymers (2 mg) were weighted out, dissolved in 2 mL of 30 mM phosphate buffer (pH = 7.4). They were then diluted to achieve the desired concentrations in the cuvette. The conditioned media (50 μL) was added and mixed into the cuvette. The solution in the cuvette was excited at 325 nm. The emission spectra's was recorded between 350 nm and 750 nm. The first peak was noticed (410 nm and 420 nm was the peak emission intensities for the **P2** and **P1** polymers respectively. Similarly a second peak developed at 510 nm and 541 nm for **P2** and **P1** respectively). Experiments were repeated 7-times to give a total of 8-runs per cell line. The same procedure was used for the unconditioned media. All fluorescent experiments were conducted on a Fluoromax-4 spectroflourimeter by HoribaJobin Yvon.

We collected three ratios for both the **P2** and **P1** polymers (**Table S-2**). These ratios were then analyzed using linear discriminant analysis to accurately quantify the fluorescent trends.

Table S-2. Ratio table from fluorescence spectral measurements. This table was generated by taking the condition cell culture media responses and dividing it by the corresponding unconditioned media responses.

Polymer	Media	Run 1	Run 2	Run 3	Run 4	Run 5	Run 6	Run 7	Run 8
P2	$PANC1_{410\ nm}$	0.847175	0.79479	0.820133	0.873235	0.963781	1.166412	1.072606	1.046227
	$PC\text{-}3_{410\ nm}$	0.980398	1.146483	1.134677	1.10082	0.845879	0.870458	0.851185	0.871067
	$22Rv1_{410\ nm}$	0.957827	1.199962	1.683281	1.747369	0.976151	1.011236	1.012318	1.04488
	$HEK\text{-}293_{410\ nm}$	1.35795	1.462229	1.533244	1.616637	1.229342	1.432922	1.467823	1.454648
	$PANC1_{510\ nm}$	1.157132	1.192934	1.136687	1.128721	1.110368	1.133213	1.133845	1.080713
	$PC\text{-}3_{510\ nm}$	1.205312	1.168119	1.118452	1.078845	1.020244	0.971663	0.977633	0.933846
	$22Rv1_{510\ nm}$	1.360548	1.312755	1.408855	1.373154	1.199632	1.068929	1.017879	1.017785
	$HEK\text{-}293_{510\ nm}$	1.205637	1.153849	1.148267	1.147307	1.13584	1.118666	1.100398	1.080768
	$PANC1_{541\ nm}$	1.214931	1.226186	1.20726	1.162033	1.178908	1.171664	1.148778	1.113138
	$PC\text{-}3_{541\ nm}$	1.20055	1.147366	1.080755	1.037216	1.036532	1.022657	0.987939	0.956024
	$22Rv1_{541\ nm}$	1.320663	1.295402	1.38728	1.306137	1.200993	1.056485	0.995993	0.974746
	$HEK\text{-}293_{541\ nm}$	1.170907	1.153743	1.135018	1.130831	1.11153	1.10938	1.083695	1.069458
P1	$PANC1_{420\ nm}$	0.754512	0.787304	0.803593	0.788134	0.752842	0.764749	0.739391	0.75971
	$PC\text{-}3_{420\ nm}$	0.793168	0.839454	0.840286	0.84325	0.837371	0.851493	0.89816	0.897751
	$22Rv1_{420\ nm}$	1.197853	1.460126	1.459727	1.515055	1.447846	1.498209	1.563769	1.550487
	$HEK\text{-}293_{420\ nm}$	1.734831	1.766465	1.841755	1.788262	1.767768	1.851178	1.846879	1.842947
	$PANC1_{523\ nm}$	1.096931	1.088802	1.054943	1.046537	1.078234	1.066194	1.048481	1.001006
	$PC\text{-}3_{523\ nm}$	1.061301	1.047744	1.046535	1.02048	1.032212	1.112304	1.069226	1.017869
	$22Rv1_{523\ nm}$	1.23598	1.26203	1.21424	1.192433	1.210153	1.190576	1.236044	1.211034
	$HEK\text{-}293_{523\ nm}$	1.234752	1.251697	1.234789	1.288396	1.248991	1.264972	1.266787	1.236204
	$PANC1_{541\ nm}$	1.129329	1.105367	1.116404	1.072364	1.116948	1.067953	1.059361	1.067068
	$PC\text{-}3_{541\ nm}$	1.080923	1.105098	1.031855	1.039193	1.049868	1.122354	1.081042	1.01804
	$22Rv1_{541\ nm}$	1.205429	1.183399	1.141565	1.13724	1.169841	1.150047	1.134717	1.181879
	$HEK\text{-}293_{541\ nm}$	1.174917	1.181515	1.185666	1.174749	1.186022	1.203861	1.209758	1.197237

Statistical Data Analysis:

An issue which potentially confounds the empirical analysis is the fact that both polymers exhibit multiple peak emission intensity ratios. Without first identifying a true peak value, any results are potentially confounded, since a given polymer found to be inferior maybe because it does not adequately discriminate between the different cell lines, or because the emission intensities recorded for the polymer-cell line pair in question were not evaluated at their maximum values. To account for this possibility, we applied LDA in a stepwise fashion. First, we applied LDA to each polymer separately, where we evaluated each potential peak value (410 nm, 510 nm and 541 nm for the **P2** polymer and 420 nm, 520 nm and 541 nm for the **P1** polymer) based on its ability to discriminate between (or predict) the four cell lines. Consistent with the **Table S-2**, each of these analyses was conducted using 32 observations (4 cell lines x 8 replications) and 4 variables (the cell line indicator and the three emission intensity wavelength variables). Once the optimal wavelengths/emission intensity ratios are established, we can proceed to the second step of our analysis, in which LDA (using the optimal wavelengths) is applied to evaluate each of the two polymers.

In a given application of LDA, the researcher has the option of using prior information to specify the predictor variables in the analysis, or using stepwise, exploratory techniques (using Wilks' Lambda and F-tests as exclusion/inclusion criteria) to identify a smaller subset set of predictor variables.[8-11] In this paper, prior information exists on the possible emission peaks. In the final LDA analysis, we also expect both polymers (**P2** and **P1**), when evaluated with LDA at their optimal wavelengths, to be included in the final LDA analysis, regardless of the use of such exclusion/inclusion criteria. As such, stepwise predictor selection criteria will not be used in the final stage of the analysis, as we expect the use of these methods to be moot (*i.e.* all predictor variables will pass the inclusion criteria). To ensure consistency across all LDA analysis, we included all candidate wavelength ratios in each of the LDA analyses used to identify the optimal emission intensity ratios.[12,13] We note in passing that we did replicate our analysis using stepwise exclusion/inclusion criteria and obtained qualitatively, but not qualitatively, similar results. More specifically, the same optimal emission intensity ratio was identified in both instances.

The use of LDA is well-established in the literature, and the reader is referred to those sources to familiarize oneself with the detailed mechanics underlying the technique.[8-13] In summary, we use standard F-tests and Wilks' Lambda values to examine mean differences across the predictor variables, and to access the fitness of the predictor variables (*i.e.* the emission intensity ratios in the first two applications of LDA or the two polymers in the final LDA) to discriminate across cell lines. Chi-square tests are used to assess the significance of any eigenvalues (and the canonical correlations and canonical discriminant functions characterized using these metrics) extracted by LDA. The overall contribution of each predictor variable to a given canonical

discriminant function can be assessed using the discriminant function coefficients and the resulting structure matrix. The contribution of each predictor to the overall LDA can be assessed using "potency indices", where larger values indicate a greater contribution to the overall model. The global fit of the LDA model can be examined using plots of the canonical discriminant functions. A useful LDA model will produce plots that clearly distinguish between the cell lines as separate groups. Lastly, internal validity is assessed by examining the percentage of cell line observations that are correctly predicted by the model. We computed predicted values using both traditional and (leave one out) cross-validation techniques. Models that correctly predict a high percentage of observations, and display consistency in predicted values across both techniques, are interpreted as having greater internal validity.

Analysis of Polymer P2:

Table S-3 provides means, F-statistics and Wilks' Lambda values for each of the **P2** polymer emission intensities, and for each cell line type. Note that smaller Wilks' Lambda values are preferred to larger values, since they indicate a greater potential for the given emission intensity to discriminate across cell lines. All F-statistics have significant p-values (less than 0.05), indicating that significant (joint) differences exist across group means for each cell lines. For the HEK cell line, the 410 nm emission intensity appears to be the highest value. The 541 nm intensity is highest for the PANC1 cell line. For the remaining cell lines, the highest mean emission intensities appear at 510 nm. Wilks' Lambda values are lowest for 410 nm, followed by 510 nm and 541 nm.

Table S-3. Tests of equality of group means

Cell Line	410 nm[a,b]	510 nm[a,b]	541 nm[a,b]
PANC1	0.948	1.134	1.178
PC-3	0.975	1.059	1.059
22Rv1	1.204	1.220	1.192
HEK	1.444	1.136	1.121
Wilks' Lambda	0.457	0.729	0.735
F-Statistic [3,28]	11.089	3.465	3.368
P-Value	<0.001	0.029	0.032

[a] first panel provides group-specific means [b] second panel provides statistics and p-values.

Table S-4 identifies the number of significant canonical correlations and canonical functions. At the 5% level, all three canonical functions are significant. The first canonical explains 63.3% of the variation across cell lines. The remaining functions explain 25.9% and 10.8%, respectively. Based on these results, we focus primarily on the first discriminant function.

Table S-4. Canonical function summary[a]

Fct.	Eigen-value	Pct. of Variance Explained	Canonical Correl.	Wilks' Lambda[a]	Chi-Square Statistic	P-Value
1	2.021	63.3	0.818	0.135[b]	55.144	<0.001
2	0.826	25.9	0.673	0.407[c]	24.739	<0.001
3	0.346	10.8	0.507	0.743[d]	8.181	0.004

[a] Lower values for Wilks' Lambda indicate greater discrimination. Wilks' Lambda and chi-square tests apply sequentially. [b] tests functions 1 – 3 cumulatively. [c] tests functions 2 – 3 cumulatively [d] tests function 3.

Figure S-1 contains a canonical function plot of the first two canonical functions (explaining 89.2% of the variation in the cell lines). Cell line 4 (HEK) is clearly distinguished as a group in the plot, but groups 1 (PANC-1), 2 (PC-3) and 3 (22Rv1) overlap slightly. Traditional and cross-validated discriminant functions each correctly predicted 62.5% and 56.3% of the cell lines, respectively, indicating a moderate degree of interval validity.

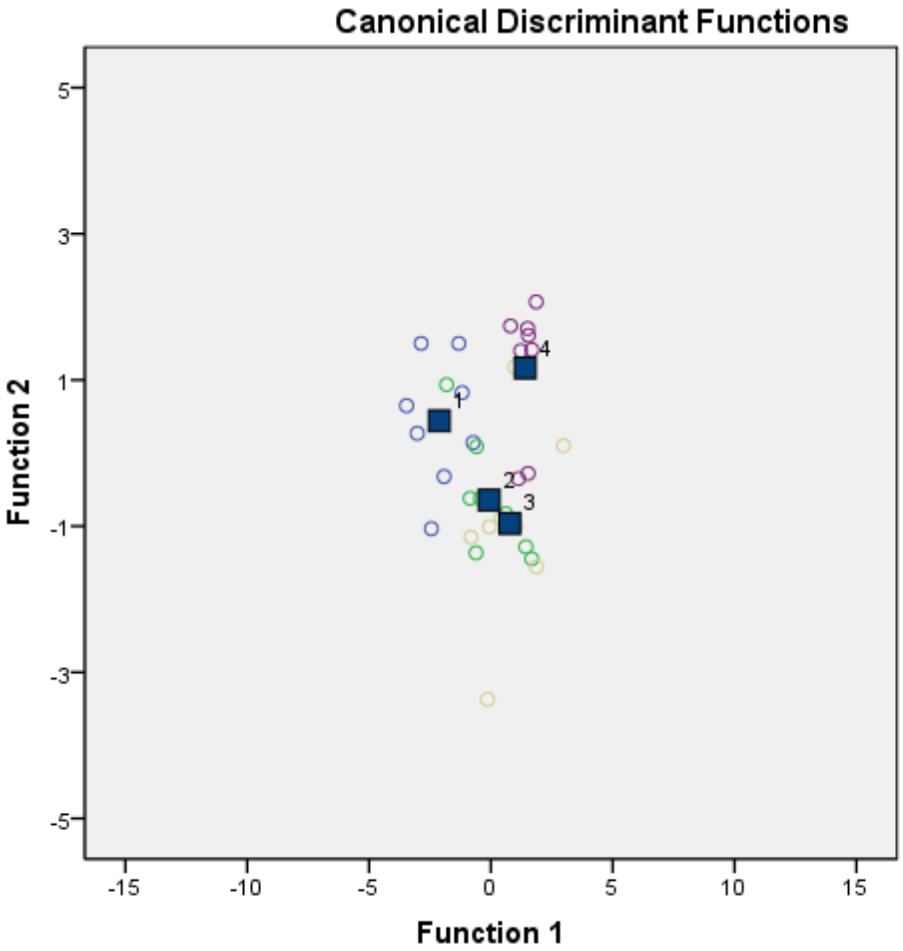

Figure S-1. Canonical correlation plot between two largest canonical correlations and each of the five cell lines: PANC1 (group 1), PC-3 (group 2), 22Rv1 (group 3) and HEK (group 4) for polymer **P2**.

Table S-5 contains the standardized discriminant function coefficients, which measure the relative contributions from each of the emission intensity to a specific discriminant function. For function 1, the 540 nm wavelength exhibits the highest coefficient in absolute value, although and 510 nm emission intensity is only slightly smaller in absolute magnitude. The 510 nm exhibits the highest value for the second function, while 540 nm has the largest coefficient for the third canonical function.

Table S-5. Standardized canonical discriminant function coefficients

Predictor	Canonical Function 1	Canonical Function 2	Canonical Function 3
410 nm	0.544	1.113	0.066
510 nm	3.191	-3.906	0.235
540 nm	-3.416	3.285	0.736

Table S-6 contains the structure matrix and the cumulative potency indices, which can be used to assess the overall contribution of each emission intensity to the discriminatory power of the LDA. The potency indices suggest that 410 nm emission intensity provides the largest overall contribution to the model's ability to distinguish between the cell lines

Table S-6. Structure matrix and potency index

Predictor	Canonical Function 1	Canonical Function 2	Canonical Function 3	Potency Index
410 nm	0.645	0.552	0.529	0.372
510 nm	-0.092	-0.014	0.996	0.113
540 nm	0.106	-0.111	0.988	0.116

Analysis of Polymer P1:

Table S-7 provides means, F-statistics and Wilks' Lambda values for each of the **P1** polymer emission intensities, and for each cell line type. All F-statistics have significant p-values (less than 0.05), indicating that significant (joint) differences exist across group means for each cell lines. For the HEK and 22Rv1 cell lines, the 420 nm emission intensity appears to be the highest value. The 541 nm intensity is highest for the PANC1 and PC-3 cell lines. Wilks' Lambda values are lowest for 420 nm, followed by 520 nm and 541 nm.

Table S-7. Tests of equality of group means

Cell Line	420 nm[a,b]	520 nm[a,b]	541 nm[a,b]
PANC1	0.769	1.060	1.092
PC-3	0.850	1.051	1.066
22Rv1	1.462	1.219	1.163
HEK	1.805	1.253	1.189
Wilks' Lambda	0.020	0.069	0.206
F-Statistic [3,28]	466.379	126.376	36.067
P-Value	<0.001	<0.001	<0.001

[a] first panel provides group-specific means [b] second panel provides statistics and p-values.

Table S-8 identifies the number of significant eigenvalues, canonical correlations and canonical functions. At the 5% level, all three canonical functions are significant. The first canonical explains 99.3% of the variation across cell lines. The remaining functions explain 0.5% and 0.2%, respectively. Based on these results, we focus primarily on the first discriminant function.

Table S-8. Canonical function summary[a]

Fct.	Eigen-value	Pct. of Variance Explained	Canonical Correl.	Wilks' Lambda[a]	Chi-Square Statistic	P-Value
1	71.429	99.3	0.993	0.009[b]	129.534	<0.001
2	0.331	0.5	0.498	0.652[c]	11.762	0.019
3	0.153	0.2	0.364	0.868[d]	3.907	0.048

[a] Lower values for Wilks' Lambda indicate greater discrimination. Wilks' Lambda and chi-square tests apply sequentially. [b] tests functions 1 – 3 cumulatively. [c] tests functions 2 – 3 cumulatively [d] tests function 3.

Figure S-2 contains a canonical function plot of the first two canonical functions (explaining 99.8% of the variation in the cell lines). All four cell lines are clearly distinguished as unique groups in the plot (although the PANC1 and PC-3 lines are relatively close together). Traditional

and cross-validated discriminant functions each correctly predicted 93.8% and 87.5% of the cell lines, respectively, indicating a reasonable degree of interval validity.

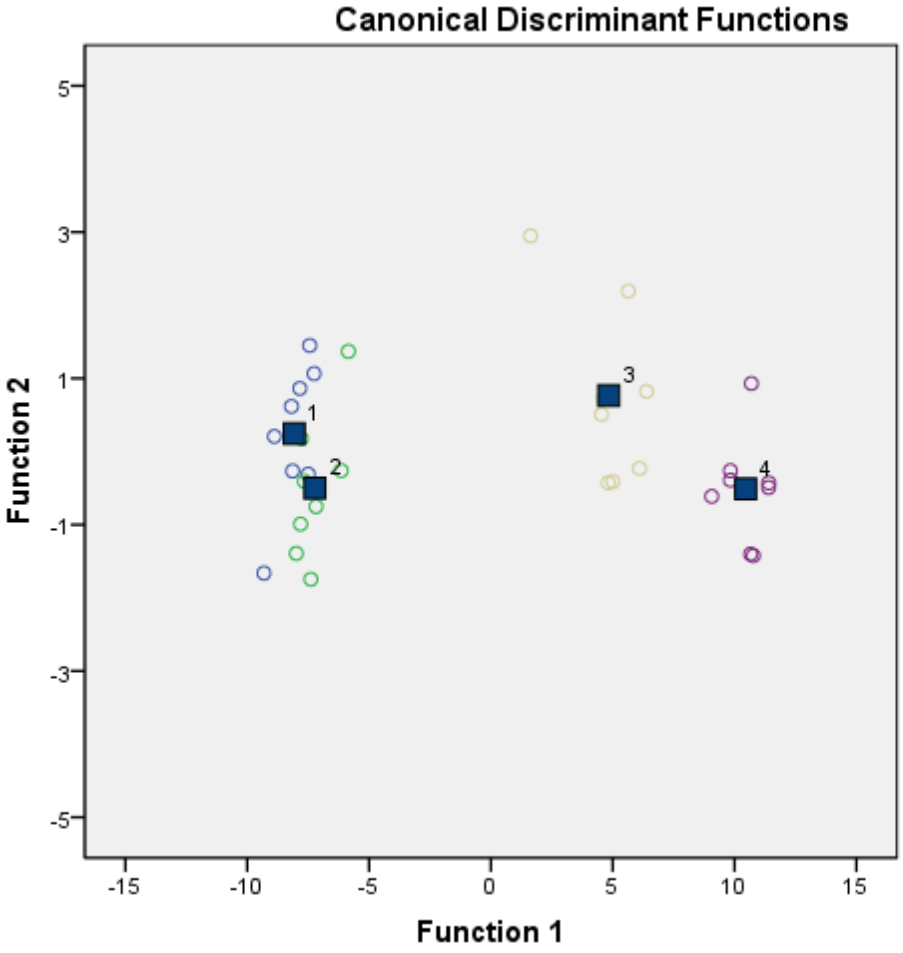

Figure S-2. Canonical correlation plot between two largest canonical correlations and each of the five cell lines: PANC1 (group 1), PC-3 (group 2), 22Rv1 (group 3) and HEK (group 4) for the polymer **P1**.

Table S-9 contains the standardized discriminant function coefficients, which measure the relative contributions of each emission intensity to a specific discriminant function. For function 1, the 420 nm wavelength exhibits the highest coefficient in absolute value. The 523 nm exhibits the highest value for the second function, while 541 nm has the largest coefficient for the third canonical function.

Table S-9. Standardized canonical discriminant function coefficients

Predictor	Canonical Function 1	Canonical Function 2	Canonical Function 3
420 nm	0.928	-0.446	0.049
523 nm	0.428	0.942	-0.781
541 nm	0.176	-0.147	1.306

Table S-10 contains the structure matrix and the cumulative potency indices, which can be used to assess the overall contribution of each emission intensity to the discriminatory power of the LDA. The potency indices suggest that 420 nm emission intensity provides the largest overall contribution to the model's ability to distinguish between the cell lines. These results should not be surprising, considering that the 420 nm variable is the primary determinant of the first canonical correlation. This variate (and its corresponding discriminant function) explains over 99% of the variation in the cell lines.

Table S-10. Structure matrix and potency index

Predictor	Canonical Function 1	Canonical Function 2	Canonical Function 3	Potency Index
420 nm	0.836	-0.522	-0.172	0.696
523 nm	0.431	0.901	0.043	0.188
541 nm	0.226	0.559	0.798	0.054

Analysis of the P2 and P1 Polymers Evaluated at Optimal Emission Intensities:

LDA was applied to each polymer (evaluated at its optimal wavelength) to determine which polymer more effectively discriminated across cell lines. As noted in **Table S-11**, standard F-tests indicate significant (joint) differences in emission intensities across the four cell lines. Interestingly, the **P1** polymer exhibits higher mean intensity values for the HEK and 22Rv1 cell lines, while the **P2** polymer exhibits higher mean values for the PANC1 and PC-3 cell lines. The P1 polymer also exhibits a lower Wilks' Lambda value, implying greater amenity to analysis through LDA.

Table S-11. Tests of equality of group means

Cell Line	**P2** Polymer (at 410 nm) [a,b]	**P1** Polymer (at 420 nm)[a,b]
PANC1	0.948	0.768
PC-3	0.975	0.850
22Rv1	1.204	1.462
HEK	1.444	1.805
Wilks' Lambda	0.457	0.020
F-Statistic [3,28]	11.809	466.379
P-Value	<0.001	<0.001

[a] first panel provides group-specific means [b] second panel provides statistics and p-values.

LDA extracted two eigenvalues, each of which can be characterized by a canonical discriminant function. The first eigenvalue explains 99.9% of the variation in the data, while the second explains the remaining 0.1%. Chi-square tests indicate that only the first of these is significant at the 5% level.

Table S-12. Canonical function summary[a]

Fct.	Eigen-value	Pct. of Variance Explained	Canonical Correl.	Wilks' Lambda[a]	Chi-Square Statistic	P-Value
1	50.022	99.9	0.990	0.019[b]	110.869	<0.001
2	0.028	0.1	0.164	0.973[c]	0.766	0.682

[a] Lower values for Wilks' Lambda indicate greater discrimination. Wilks' Lambda and chi-square tests apply sequentially. [b] tests functions 1 – 3 cumulatively. [c] tests functions 2 – 3 cumulatively [d] tests function 3.

A global assessment of the overall LDA model's fit can be made by examining **Figure S-3**, which displays a plot of the two canonical discriminant functions. Note that cell lines 3 and 4

are clearly and distinctly grouped, implying that the LDA does an acceptable job of identifying these cell lines from the data. Groups 1 and 2 are discernable as groups, but are not distinctly separated from each other. As such, the LDA model can distinguish between prostate cancer cell lines (22Rv1 and PC-3), but interestingly enough does not do an acceptable job in distinguishing between pancreatic (PANC1) and prostate cancer (PC-3) cell lines. Traditional and cross-validated LDA methods predicted 96.9 and 93.8 of the observations, respectively.

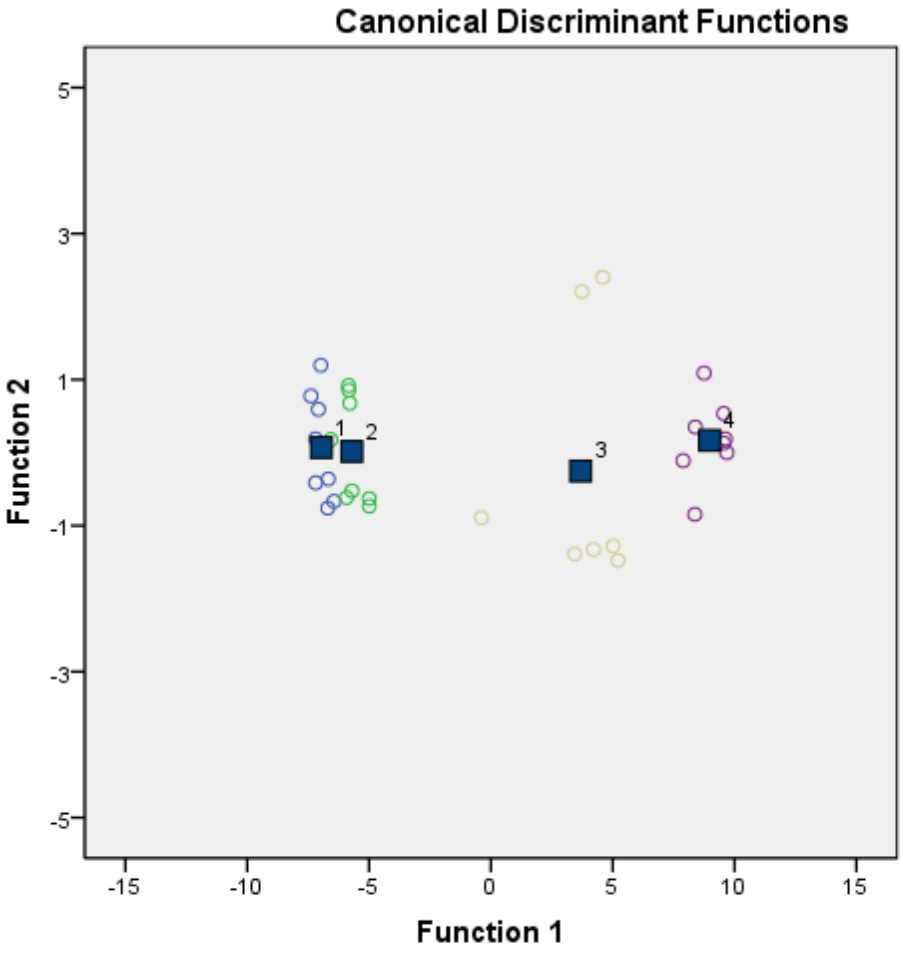

Figure S-3. Canonical correlation plot between two largest canonical correlations and each of the five cell lines: PANC1 (group 1), PC-3 (group 2), 22Rv1 (group 3) and HEK (group 4).

Examination of the structure matrix coefficients suggests that the **P2** polymer contributes relatively more towards the formation of the second canonical discriminant function (note the relatively large coefficient value for Canonical Function 2), while the **P1** polymer primarily contributes to the formation of the first canonical function. The potency index is much larger for the **P1** polymer than the **P2** polymer, suggesting that the **P1** is, in fact, the polymer which

provides the best discrimination across the cell lines. These results are intuitive, considering that the **P1** polymer contributed primarily to the formation of the first canonical function, whose eigenvalue explained 99.9% of the variation in the LDA model.

Table S-13. Standardized canonical discriminant function coefficients

Predictor	Canonical Function 1	Canonical Function 2
P2 Polymer	0.033	1.007
P1 Polymer	0.996	-0.153

Table S-14. Structure matrix and potency index

Predictor	Canonical Function 1	Canonical Function 2	Potency Index
P2 Polymer	0.152	0.988	0.024
P1 Polymer	0.999	-0.032	0.997

References:

(1) Dutta, R.; Scott, M. D.; Haldar, M. K.; Ganguly, B.; Srivastava, D. K.; Friesner, D. L.; Mallik, S. *Bioorg Med Chem Lett* **2011**, *21*, 2007.

(2) Sramkoski, R. M.; Pretlow, T. G., 2nd; Giaconia, J. M.; Pretlow, T. P.; Schwartz, S.; Sy, M. S.; Marengo, S. R.; Rhim, J. S.; Zhang, D.; Jacobberger, J. W. *In Vitro Cell Dev Biol Anim* **1999**, *35*, 403.

(3) Kim, H. J.; Park, Y. I.; Dong, M. S. *Toxicol In Vitro* **2006**, *20*, 1159.

(4) Mazor, M.; Kawano, Y.; Zhu, H.; Waxman, J.; Kypta, R. M. *Oncogene* **2004**, *23*, 7882.

(5) Lieber, M.; Mazzetta, J.; Nelson-Rees, W.; Kaplan, M.; Todaro, G. *Int J Cancer* **1975**, *15*, 741.

(6) Liu, H.; Chen, B.; Lilly, B. *Angiogenesis* **2008**, *11*, 223.

(7) Harris, J. E.; Friedland, J. S. *J Neurosci Methods* **2008**, *173*, 291.

(8) Miranda, O. R.; Creran, B.; Rotello, V. M. *Curr Opin Chem Biol* **2010**, *14*, 728.

(9) Bunz, U. H.; Rotello, V. M. *Angew Chem Int Ed Engl* **2010**, *49*, 3268.

(10) Bajaj, A.; Miranda, O. R.; Phillips, R.; Kim, I. B.; Jerry, D. J.; Bunz, U. H.; Rotello, V. M. *J Am Chem Soc* **2010**, *132*, 1018.

(11) Nyren-Erickson, E. K.; Haldar, M. K.; Gu, Y.; Qian, S. Y.; Friesner, D. L.; Mallik, S. *Anal Chem* **2011**, *83*, 5989.

(12) Johnson, R. A.; Wichern, D. W. *Applied multivariate statistical analysis*; 5th ed.; Prentice Hall: Upper Saddle River, N.J., 2002.

(13) Hair, J. F. *Multivariate data analysis*; Prentice Hall: Upper Saddle River, N.J., 1998.